

Modeling and Dynamic Performance Analysis of PMBLDC Motor

Dr. Jamal A. Mohammed*

Received on: 25 /1/2010

Accepted on:7/10/ 2010

Abstract

Permanent Magnet Brushless DC (PMBLDC) motors are one of the electrical drives that are rapidly gaining popularity, due to their high efficiency, good dynamic response, high mechanical power density, simplicity, cost effectiveness and low maintenance.

In this paper, the state-space technique is presented and used for analyzing the dynamic performance of PMBLDC motor. The method is based on the formulation of state equations from the mathematical model of the motor and conversion of them into a set of linear algebraic equations by the use of trapezoidal rule of integration. The simulation of the motor has been done using the software package Matlab.

Keywords: PMBLDC motor, Trapezoidal, torque pulsation.

نمذجة وتحليل الأداء الديناميكي لمحرك التيار المستمر ذو المغناطيس الدائم والخالي من الفرش الكربونية

الخلاصة

محركات التيار المستمر ذو المغناطيس الدائم والخالية من الفرش الكربونية هي أحد المسوقات الكهربائية التي اكتسبت شعبية كبيرة بسبب كفاءتها العالية واستجابتها الديناميكية الجيدة وامتلاكها الكثافة العالية للقدرة الميكانيكية وبساطتها وفاعلية الكلفة وانخفاض صيانتها. في البحث الحالي تم تمثيل واستخدام تقنية فراغ الحالة لتحليل الأداء الديناميكي لمحرك التيار المستمر ذو المغناطيس الدائم والخالي من الفرش الكربونية. هذه الطريقة تعتمد على تشكيل معادلات الحالة من النموذج الرياضي للمحرك وتحويلها إلى مجموعة من المعادلات الجبرية الخطية باستخدام القاعدة الرباعية للتكامل. تمت محاكاة المحرك الحالي باستخدام الحقيبة البرمجية Matlab.

1. Introduction

In modern electrical machines industry productions, the brushless DC (BLDC) motors are rapidly gaining popularity. As the name implies, BLDC motors do not use brushes for commutation; instead, they are electronically commutated. BLDC motors have advantages over brushed DC motors and induction motors. They

have better speed versus torque characteristics, high dynamic response, high efficiency, long operating life, noiseless operation, higher speed ranges, and rugged construction. Also, torque delivered to the motor size is higher, making it useful in applications where space and weight are critical factors. With these advantages, BLDC motors find wide spread applications in

* Electromechanical Engineering Department, University of Technology/Baghdad

automotive, appliance, robot, aerospace, consumer, medical, electric traction, road vehicles (Hybrid Electric Vehicles HEVs and Electric Vehicles EVs), aircrafts, military equipment, hard disk drive, HVAC, instrumentation and automation industries [1,2].

Permanent Magnet motors can be classified into two categories: permanent magnet synchronous (PMS) motor and permanent magnet brushless DC (PMBLDC) motor. These motors have many similarities. They both have permanent magnets on the rotor and require alternating stator currents to produce constant torque. The difference between them is that the PMS motor has a sinusoidal back-*emf* while the BLDC motor has a trapezoidal back-*emf*. This leads to different operating and control requirement for these two machines [2].

The dynamic modeling and simulation of PMBLDC motor has been widely studied because of their increasing usage in industrial automation. It is therefore necessary to analyze the dynamic characteristics of this motor in order to control it, simulate it, and to evaluate its performance.

PMBLDC motor has been a topic of interest for the last twenty years. Some authors have carried out modeling and simulation of such motors. In [3], the dynamic models and equivalent circuits of two PM motors (PMS and BLDC) had been presented using the d, q-model. In [4], a unified approach of Bond graph for modeling of 3-phase BLDC motor and its drive circuit was used and analyzed. In [5], the performance of a 3-phase PM motor

operating as a synchronous and BLDC motor had been analyzed using software package Matlab/Simulink. In [6], modeling of 3-phase BLDC motor with Matlab/Simulink package program was presented. This model can be providing a guide in the modeling of this motor.

All the above papers were used the conventional modeling methods which involve more computational work.

The aim of this paper is to make a model that would be simple, accurate, easy to modify and suitable for real time implementation.

When the current paper is compared to the previous developed approaches, the proposed model used is different: *i)* it is converted into discrete time form where *Trapezoidal* algorithm is used, *ii)* it is independent of the number of motor phases, *iii)* it eliminates numerical problems, reduces simulation times significantly and there is no convergence problem, and *iv)* it has minimal number of parameters.

The dynamic behavior of PMBLDC motor has been studied in this paper and the results indicate that this motor can be subject to severe torque pulsations due to the stator currents commutating from one phase to another. This phenomenon can affect the motor performance of torque and speed.

In this paper, a new Matlab simulation method based on developed *Trapezoidal* algorithm for the dynamic performance analysis is put forward on the base of the state-space mathematical model of the PMBLDC motor.

2. Basic Construction and Operation:

PMBLDC motor is a type of synchronous motor. This means that the magnetic field generated by the stator and the magnetic field generated by rotor rotate at the same frequency.

PMBLDC motors come in 1-phase, 2-phase and 3-phase configurations. Corresponding to its type, the stator has the same number of windings. Out of these, 3-phase is the most popular and widely used. Most PMBLDC motors have three stator windings connected in star fashion.

There are two types of stator winding variants, which are trapezoidal and sinusoidal motors. The differentiation based on the interconnection of coils in the stator windings to give the different types of back-*emf*. The rotor is a surface-mounted design which made of permanent magnet and can vary from two to eight pole pairs.

Each commutation sequence has one of the windings energized to positive power (current enters into the winding), the second winding is negative (current exits the winding) and the third is in a non-energized condition. Torque is produced because of the interaction between the magnetic field generated by the stator coils and the permanent magnet. In order to keep the motor running, the magnetic field produced by the winding shift position as the rotor moves to catch up with the stator field [2].

3. Mathematical (Dynamic) Model:

State variable model is mathematical model which created from analysis of PMBLDC motor characteristic. From the state variable, the mathematical model [3,6] is

converted by using [7,8] into discrete time form where *trapezoidal* algorithm is used. The trapezoidal is the preferred algorithm because of its highest accuracy level and lowest simulation time. A combination of the forward and backward-Euler algorithms generates the trapezoidal algorithm. Trapezoidal algorithm is a technique usually used to evaluate differential of bounded functions [9].

State variable model is also known as state-space model. Advantages of the state-space method over the existing methods are that no convergence, initialization, instability problems, and no restrictions such as the number and configuration of nonlinear elements. This model needs to be transformed to discrete time because differential equation in state-space can be solved easily.

Developing the model of PMBLDC motor is to investigate torque behavior. When the input currents and motor flux linkages are perfect, no torque pulsations are produced in the motor. However imperfections in the currents arise due to finite commutation time while imperfections in the flux linkage can arise due to the phase spread, finite slot numbers and manufacturing tolerances [10].

Since both the magnet and the stainless steel retaining sleeves of the PMBLDC motor have high resistivity, rotor induced currents can be neglected and no damper windings are modeled.

Because of the fact that the induced *emfs* are non-sinusoidal in this motor, phase variables are chosen for the model development.

For a symmetrical windings and balanced system of PMBLDC motor

shown in Fig. 1, the voltage equation across the motor winding is as follows: Applying Kirchhoff's voltage law for the 3-phase stator loop winding circuit's yields [11]:

$$\begin{aligned} V_a &= R_a I_a + L_a \frac{dI_a}{dt} + L_{ab} \frac{dI_b}{dt} + L_{ca} \frac{dI_c}{dt} + e_a \\ V_b &= R_b I_b + L_b \frac{dI_b}{dt} + L_{ab} \frac{dI_a}{dt} + L_{bc} \frac{dI_c}{dt} + e_b \\ V_c &= R_c I_c + L_c \frac{dI_c}{dt} + L_{ac} \frac{dI_a}{dt} + L_{bc} \frac{dI_b}{dt} + e_c \end{aligned} \quad (1)$$

, where the back-*emf* waveforms e_a , e_b and e_c are functions of angular velocity ω of the rotor shaft, so: $e=K_e \omega$, where K_e is the back-*emf* constant. V_a , V_b and V_c are stator phase voltages. I_a , I_b and I_c are stator phase currents. R_a , R_b and R_c are winding phase resistances. L_a , L_b and L_c are phase self inductances. L_{ab} , L_{bc} and L_{ca} are mutual inductances between phases.

From the basic equation above, the matrix dimension circuit equation of 3-phase windings in phase variables are:

$$\begin{aligned} \begin{bmatrix} V_a \\ V_b \\ V_c \end{bmatrix} &= \begin{bmatrix} R_s & 0 & 0 \\ 0 & R_s & 0 \\ 0 & 0 & R_s \end{bmatrix} \begin{bmatrix} I_a \\ I_b \\ I_c \end{bmatrix} \\ &+ p \begin{bmatrix} L_{aa} & L_{ab} & L_{ac} \\ L_{ba} & L_{bb} & L_{bc} \\ L_{ca} & L_{cb} & L_{cc} \end{bmatrix} \begin{bmatrix} I_a \\ I_b \\ I_c \end{bmatrix} + \begin{bmatrix} E_a \\ E_b \\ E_c \end{bmatrix} \end{aligned} \quad \dots(2)$$

The analysis of motor is based on the following assumptions for simplification and accuracy: 1) back *emf*'s E_a , E_b and E_c are having a trapezoidal shape characteristic, 2) Saturation, Eddy currents and Hysteresis losses are negligible and 3) there is no change in rotor reluctance with angle (uniform air-gap), which makes the total stator current is

constrained to be balanced and the self and mutual inductances of the stator are constant values which leads to simplification of the inductance matrix in the model as:

$$\begin{aligned} \begin{bmatrix} V_a \\ V_b \\ V_c \end{bmatrix} &= R_s \begin{bmatrix} 1 & 0 & 0 \\ 0 & 1 & 0 \\ 0 & 0 & 1 \end{bmatrix} \begin{bmatrix} I_a \\ I_b \\ I_c \end{bmatrix} \\ &+ p \begin{bmatrix} L-M & 0 & 0 \\ 0 & L-M & 0 \\ 0 & 0 & L-M \end{bmatrix} \begin{bmatrix} I_a \\ I_b \\ I_c \end{bmatrix} + K_u \begin{bmatrix} w_a \\ w_b \\ w_c \end{bmatrix} \end{aligned} \quad \dots(3)$$

Hence the state-space forms are:

$$\begin{aligned} \frac{d}{dt} \begin{bmatrix} I_a \\ I_b \\ I_c \end{bmatrix} &= \begin{bmatrix} -\frac{R_s}{L_1} & 0 & 0 \\ 0 & -\frac{R_s}{L_1} & 0 \\ 0 & 0 & -\frac{R_s}{L_1} \end{bmatrix} \begin{bmatrix} I_a \\ I_b \\ I_c \end{bmatrix} + \\ \begin{bmatrix} \frac{1}{L_1} & 0 & 0 \\ 0 & \frac{1}{L_1} & 0 \\ 0 & 0 & \frac{1}{L_1} \end{bmatrix} \begin{bmatrix} V_a \\ V_b \\ V_c \end{bmatrix} - \begin{bmatrix} \frac{K_u}{L_1} & 0 & 0 \\ 0 & \frac{K_u}{L_1} & 0 \\ 0 & 0 & \frac{K_u}{L_1} \end{bmatrix} \begin{bmatrix} w_a \\ w_b \\ w_c \end{bmatrix} \end{aligned} \quad \dots(4)$$

, where $L_1=L-M$, L and M are the self and mutual inductances, respectively, and ω_a , ω_b , and ω_c are the angular speeds for electrical quantities of phases a , b and c , respectively.

The state form equations above have been derived as in the Appendix and implemented in Matlab software to find the stator currents. The stator currents then used to find the electromechanical torque T_e as follows:

$$T_e = [E_a I_a + E_b I_b + E_c I_c] / w_m \quad \dots(5)$$

, where ω_m is a rotor speed. To find the solution for the stator current and electromechanical torque, the

specification has been given in Table 1 in the Appendix.

The mechanical dynamic equation is:

$$J \left(\frac{dw}{dt} \right) + B_m w = T_e - T_L \quad [3,6] \quad \dots(6)$$

, where J is moment inertia, B_m is a damping coefficient and T_L is a load torque. Combining all the pervious equations, the system space form in Eq. 4, becomes:

$$\dot{x} = Ax + Bu + Ew \quad \dots(7)$$

, where $x = [I_a \ I_b \ I_c]^t$, $u = [V_a \ V_b \ V_c]^t$,

$$\omega = [\omega_a \ \omega_b \ \omega_c]^t, A = \begin{bmatrix} -\frac{R_s}{L_1} & 0 & 0 \\ 0 & -\frac{R_s}{L_1} & 0 \\ 0 & 0 & -\frac{R_s}{L_1} \end{bmatrix},$$

$$B = \begin{bmatrix} \frac{1}{L_1} & 0 & 0 \\ 0 & \frac{1}{L_1} & 0 \\ 0 & 0 & \frac{1}{L_1} \end{bmatrix}, \text{ and } E = - \begin{bmatrix} \frac{K_u}{L_1} & 0 & 0 \\ 0 & \frac{K_u}{L_1} & 0 \\ 0 & 0 & \frac{K_u}{L_1} \end{bmatrix}$$

The discrete-time form of the above model is obtained by sampling and clamping the input at the time intervals kT . Then the model may be arranged in the form suitable for *Trapezoidal algorithm* [9] as follow:

$$x(k+1) = \left(I - \frac{T}{2} A \right)^{-1} \begin{bmatrix} \left(I - \frac{T}{2} A \right) x(k) + \\ \frac{T}{2} B [u(k+1) + u(k)] + \\ \frac{T}{2} E [w(k+1) + w(k)] \end{bmatrix} \quad (8)$$

All the above equations are derived as in the Appendix.

By using the specification from Table A in the Appendix and Eq.8, the

dynamic performance of PMLDLC motor has been analyzed by using Matlab simulation.

Developing the equation from 3-phase PMLDLC motor until calculation of state-space form has been done by manual calculation, while stator current and electromechanical torque has been calculated by Matlab simulation.

4. Torque Production:

The back-emf and the required currents in order to produce constant torque are shown in Fig. 2 in an ideal machine. In Eq. 5, it was shown that the torque is given by the product of the back-emf and stator current waveform divided by the speed. The backemf divided by the speed is a constant and represents the flux linkage λ which has the same waveform as the backemf in Fig. 2. The flux linkage is horizontal (constant) for 120° and for constant torque, it is necessary to supply a rectangular shaped current to the phase during this period. When the flux linkage is negative, a negative current is needed in order to produce constant positive torque.

In addition, at any given instant, only two phases conduct current with the phase carrying the positive current using the phase carrying the negative current as a return path. In Fig. 2, consider an instant when:

$$\begin{aligned} e_a &= E_p; & e_b &= -E_p \\ i_a &= I_p; & i_b &= -I_p; & i_c &= 0 \end{aligned} \quad \dots(9)$$

The electromechanical torque becomes:

$$T_e = (E_p I_p + E_p I_p) / \omega_r = 2E_p I_p / \omega_r = 2\lambda_p I_p \quad \dots(10)$$

At any other instant, it will always be found from Fig. 2 that only two

phases conduct, with the third being zero and then Eq. 10 holds. The torque predicted from this idealized machine is therefore constant with no torque pulsations.

Any periodic wave can be expressed as a Fourier series. Hence both the flux linkage and current waveforms can be expressed as a Fourier series as well.

It is known that current and flux linkage harmonics of the same order interact to produce constant torque while if they are of different orders they produce pulsating torques [10].

The steady torque is given by the interaction of the fundamental of the flux linkage with the fundamental component of current plus the 5th harmonic of the flux with the 5th harmonic of current etc. That is all odd harmonics of flux which interact with current harmonics of the same order (except triplen) produce a constant torque.

In practice, deviations from the idealized current and flux linkage waveforms shown in Fig. 2 occur.

In a practical machine, it is impossible to force a rectangular current to flow into the machine windings. This is because the motor inductance limits the rate of change of current. In the steady-state, the rise time of the current depends on the voltage differential between the input dc and the backemf, and the time constant of the stator winding which is given by the ratio of the stator leakage inductance to resistance. The higher this ratio, the longer is the rise time of the current. Therefore, the torque ripple results from the motor currents or flux linkage deviating from the ideal [10].

5. Torque Ripple

The biggest disadvantage of the BLDC motor drive configuration is the physical inability to generate the ideal rectangular pulse currents. As shown in the Fig. 2, the currents must make the required transitions instantaneously. In reality, the transitions require finite time. As a result, torque ripple is created at each commutation on point during the finite transition time of each phase current. This torque ripple is known as *commutation torque ripple*.

In addition to significant commutation torque ripple, the BLDC motor configuration produces torque ripple whenever the backemf or current shapes deviate from their ideal characteristics shown in Fig. 2.

Because torque ripple is difficult to eliminate in the BLDC motor configuration, it is seldom used in applications where minimum torque ripple is required. However, in velocity applications such as fans and pumps where motor speed and inertia are sufficiently high, torque ripple has little affect because of the inherent filtering provided by the inertia [12].

6. Results and Discussion:

The performance analysis of the PMLDC motor is the final stage of Matlab programming where the plot curve or graph has been displayed. The expected graphs are phase stator currents versus time, torque versus time and torque versus speed, torque spectra and the effect of the time constant T on the motor behavior.

Fig. 3, show the simulation results of the phase currents of the proposed motor with different values of per unit motor time constant T ; (where the base

value of $T=L_1/R_s=0.0779$ Sec). It can be seen from the figures that there is some amount of ripple in the current waveforms due to finite commutation time, since the motor inductance limits the rate of change of current. Increasing of T (or L) causes increase of the motor impedance with frequency $X=2\pi fL$; therefore the harmonic currents (especially higher orders) decrease. As result, the ripple in the instantaneous current will decrease with increasing L or T from (0.25 to 2) p.u.

It must be noted that the increase in T causes increase in the motor ratings, so the current amplitude will increase too.

Because of the nonrectangular current, torque pulsations are produced during the commutation of the currents as shown in Fig. 4. The results presented show the effects of changing per unit T on the overall magnitude of the torque pulsations. The figure shows that the average torque increases with T while the torque ripple decreases with T since the current ripple decreases too.

A Matlab program is written to determine the output torque spectra corresponding for the torque waveforms shown in Fig. 5. From this figure, it is clear that there is a reduction in the torque harmonics as the order increases because the more effect of L (or X) on the higher order harmonics, so that the contribution of the higher order harmonics to the steady torque is negligible.

A plot of the average torque versus T is given in Fig. 6. It can be seen that increasing T causes linear increase in the developed electromagnetic torque T_e , since the increase in T means increase in the motor ratings. On the other side, the increase in T (or L)

causes decrease in the torque ripple due to decreasing the distortion in the current waveform which was aforementioned and as a result decrease in the percentage per unit torque ripple (where base torque average is $T_{av}=2.243$ N.m.) as shown in Fig. 7.

The motor speed waveforms with different values of input voltages (8, 10, and 12 V) are shown in the Fig. 8. The speed increases with voltage increase. These figures show how the ripple appears in the speed waveforms due to the existing of the ripple in torque and decreases with the increase of T .

A simplified of the relationship of motor speed N and torque T_e derived as in Eq. A. 16 in the Appendix can be plotted as in the Fig. 9 for different values of input voltages (8, 10, and 12 V). The torque-speed characteristics in Fig. 9 show the inverse linear proportion between N and T_e according to the Eq. A. 16. These characteristics form series of straight lines and the slope of these lines decreases with T increase. Also, it can be seen how the speed increases with the input voltage.

7. Conclusions:

In this paper, a numerical simulation method using Trapezoidal algorithm for modeling and analyzing the dynamic performance of 3-phase PMSM motor and overcoming the drawbacks of the conventional modeling approaches have been used.

The aim of this paper is to make a model simple, accurate, easy to modify has flexible structure and enables to users to change motor parameters easily and suitable for real time implementation. The simulation results

of this work have shown that these goals have been achieved.

The developed model can produce precise prediction of motor performance during transient as well as steady-state operation. Therefore, the mechanism of phase commutation and generation of torque ripple can be easily observed and analyzed in this model.

It is shown that, a constant output torque is produced only if the flux density and current waveforms of the motor are idealized. The results show that, because of the nonrectangular current, torque pulsations are produced during the commutation of current and depend on time constant of the motor.

The results indicate the suitability of using a Fourier series to examine the torque behavior in the PMBLDC motor. From the results presented earlier, the motor torque pulsations clearly decrease nonlinearly as a function of motor time constant, while the motor has linear relationship between the magnitude of average torque and time constant.

Torque-speed characteristics form series of straight lines. This shows that inductance present in the armature played no part in affecting its shape.

Increasing torque leads to drop in speed. Since the flux of motor is constant, then speed of motor depends on only armature supply.

The flat torque-speed characteristics of the motor enable operation at all speeds with rated load and produce predictable speed regulation. Thus motor can rotate with wide range of speeds.

The results show that the motor has approximately constant torque-speed

characteristics at higher values of time constant.

8. References:

- [1] S. S. Bharatkar, R. Yanamshetti, D. Chatterjee, and A. K. Ganguli, Performance Comparison of an efficient IM Controller and BLDC Drive for Vehicular Applications, *Journal of Modelling and Simulation of Systems* (Vol.1-2010/Iss.3), pp. 187-193.
- [2] Microchip Technology, Brushless DC (BLDC) Motor Fundamentals, Application Note, AN885, 2003.
- [3] P. Pillay and R. Krishnan, "Modeling, simulation, and analysis of permanent-magnet motor drives, part II: The brushless DC motor drive," *IEEE Trans. on Industry Applications*, Vol. 25, No. 2, pp. 274-279, 1989.
- [4] P. Vaz, PS. S. Dhama and S. Trivedi, Bond Graph Modeling and Simulation of Three-phase PM BLDC Motor, 14th National Conf. on Machines and Mechanisms, NIT, Durgapur, India, Dec. pp. 17-18, 2009.
- [5] S. Sekalala, Performance of a Three-phase Permanent Motor Operating as a Synchronous Motor and a Brushless DC Motor, MSc. Thesis, City University, New York, Aug., 2006.
- [6] C. Gencer and M. Gedikpinar, "Modeling and Simulation of BLDCM using Matlab/Simulink", *Journal of Applied Sciences* 6(3), 688-691(2006).
- [7] Naresh K. Sinha, "Identification of continuous-time systems from samples of input-output data: An introduction", *Sādhanā Journal*, Vol. 25, No. 2, April 2000, pp. 75-83.
- [8] R. Stengel, Continuous- and Discrete-Time Dynamic Models,

- Robotics and Intelligent Sys. MAE 345, Report, Princeton University, 2007.
- [9] D. Houcque, Applications of Matlab: Ordinary Differential Equations (ODE), Northwestern University, Report, 2006, pp. 1-12.
- [10] P. Pillay and R. Krishnan, "An investigation into the torque behavior of a brushless DC motor," IEEE IAS Ann. Meeting, New York, pp. 201-208, 1988.
- [11] Krishnan, R.: Electric Motor Drives: Modeling, Analysis, and Control, (2006), Prentice Hall, India.
- [12] J. F. Gieras and M. E. Marler, Analytical Prediction of Torque Ripple in Permanent Magnet Brushless Motors, 15th Int. Conference on Electrical Machines, August, 2002.

Table A: Specification of PMBLDC motor modeling

Parameters	Value
Stator Resistor, R_s	0.7 Ω
Self Inductance, L	40mH
Mutual Inductance, M	3.67mH
Voltage per-phase, V	12V
Torque Load, T_L	2.21 N-m
Rms Phase Current, I_s	1 A
Speed, N	125 RPM
Back-emf Constant, K_e	1.257 V/rad/s
Torque Constant, K_t	0.76 N-m/A
Moment of Inertia, J	0.0025 kg-m ²
Damping Coefficient, B_m	0.0237 N-m/RPM

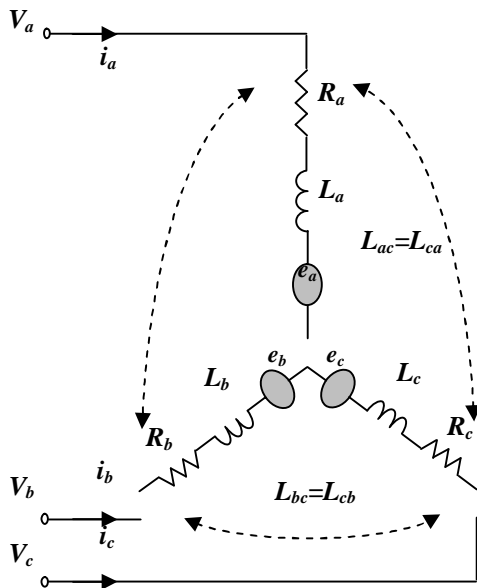


Figure (1) PMBLDC motor equivalent circuit for dynamic equations

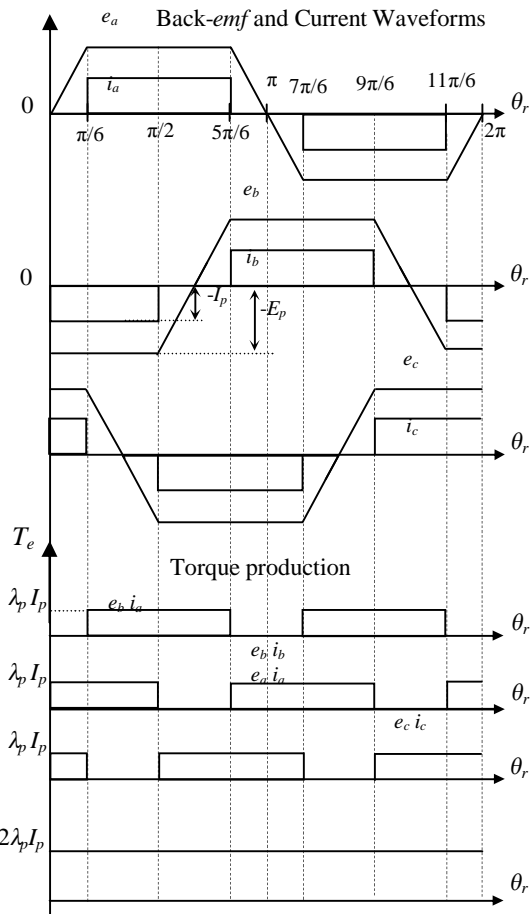


Figure (2) Back-emf and current waveforms and torque production in trapezoidal PMBLDC motor

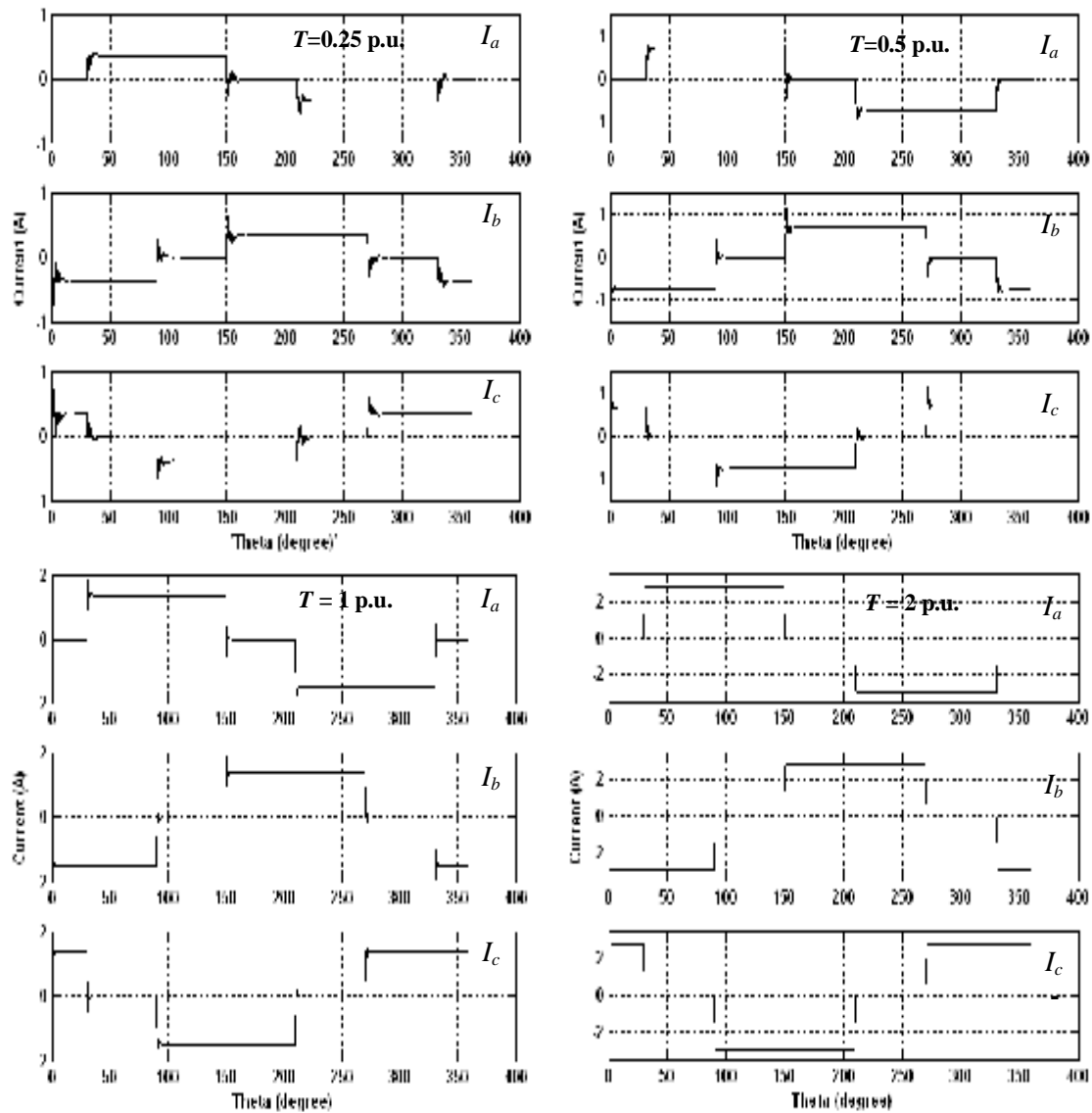


Figure (3) Phase currents as a function of rotation angle with different values of time cons. T

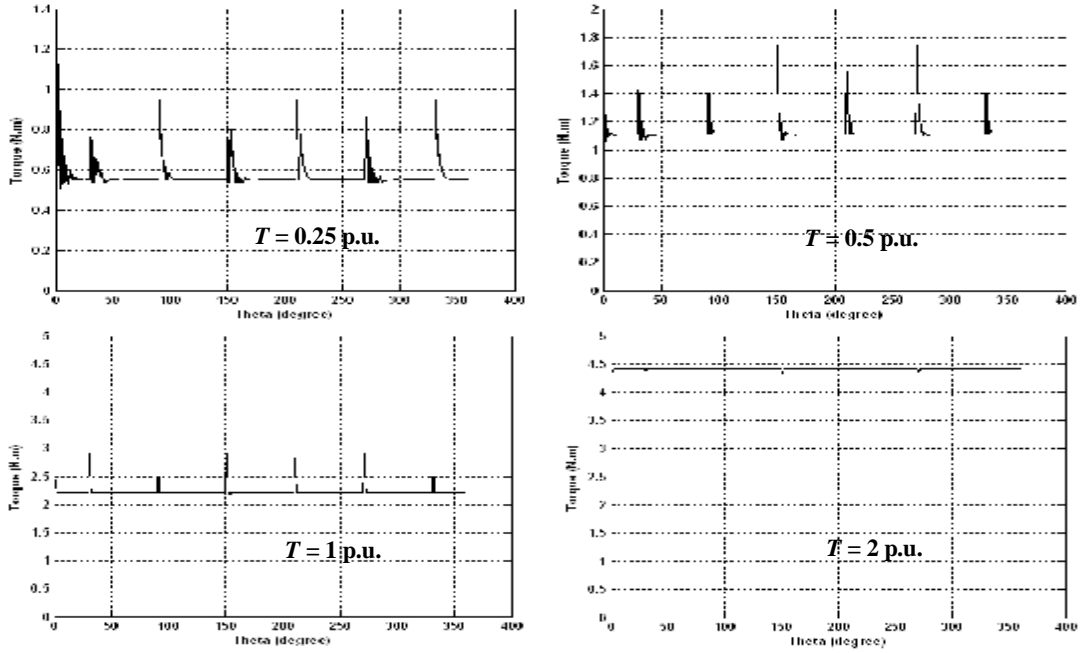


Figure (4) Electromagnetic torque as a function of rotation angle with different values of time const. T , (where the Torque load; $T_L=2.21$ N.m)

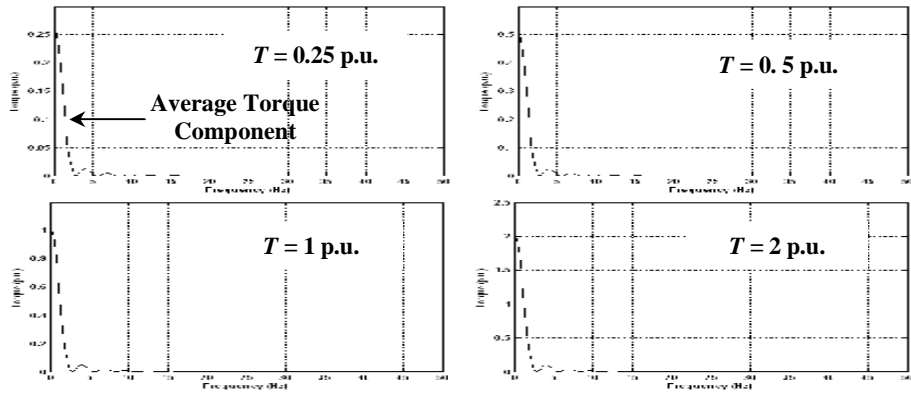


Figure (5) Torque spectra with different values of time const T

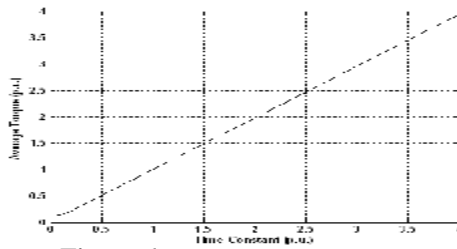


Figure 6: p.u. average torque vs. p.u. time const. T

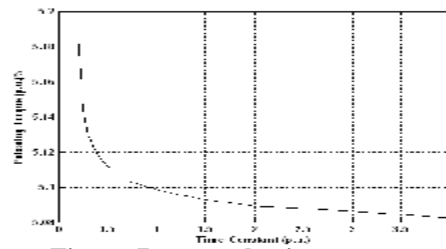


Figure 7: p.u. pulsating torque vs. p.u. time const. T

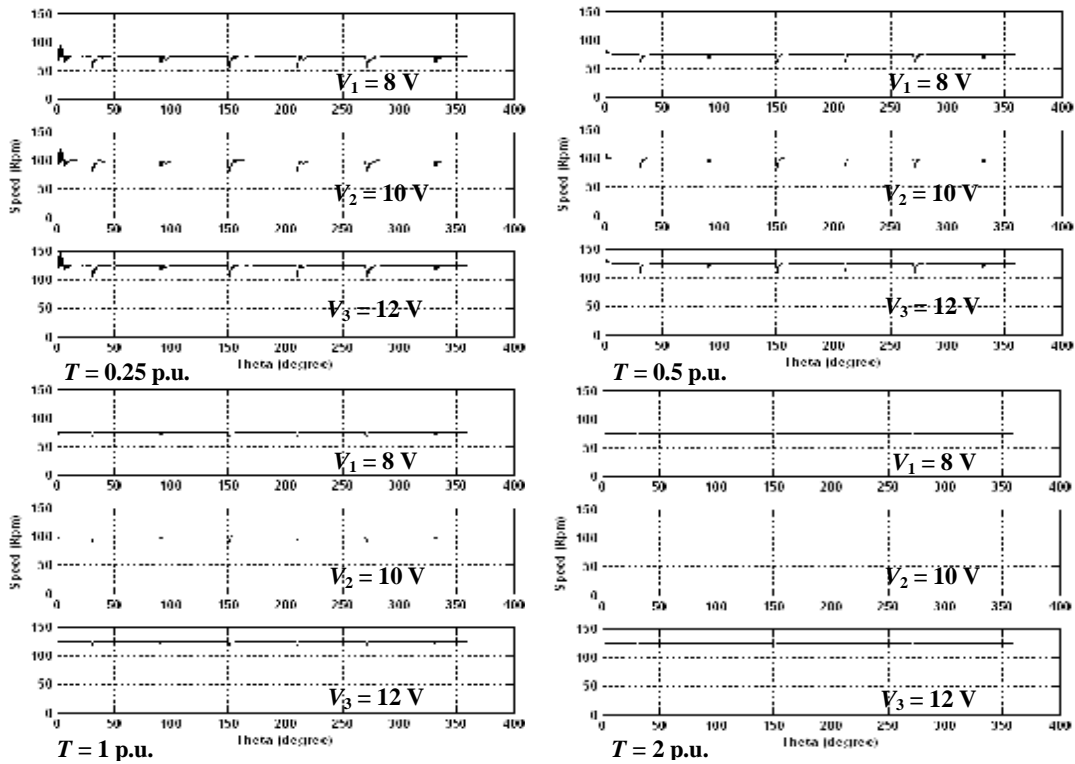


Figure (8) Motor speeds N at different input voltages V and time const. T

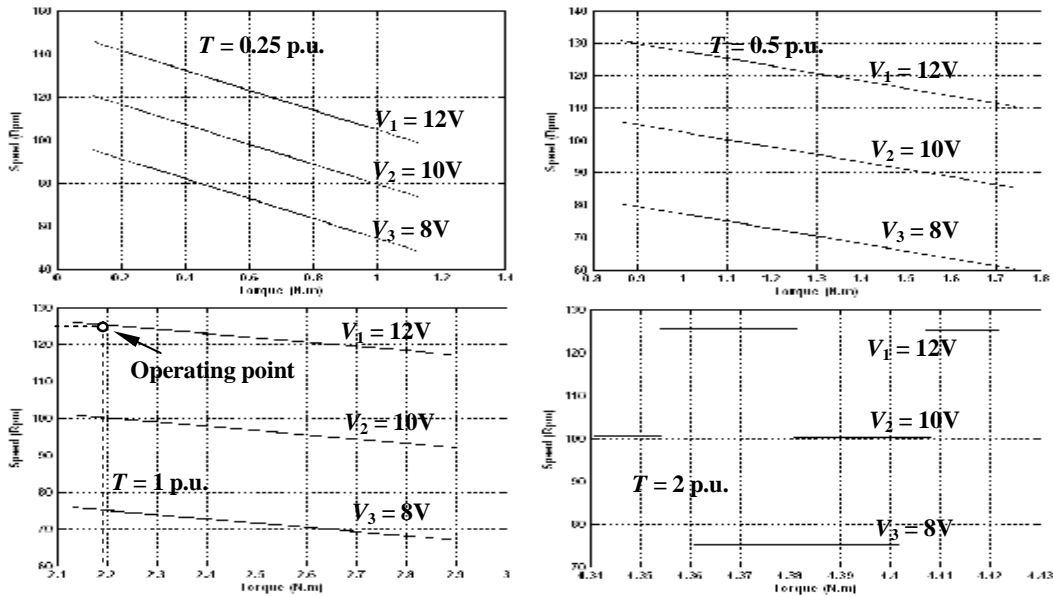


Figure (9) Speed N vs. electromagnetic torque at different input voltages V and time const. T [Operating point; $V = 12\text{ V}$, $T_e = 2.21\text{ N}\cdot\text{m}$ & $N = 125\text{ RPM}$]

Appendix

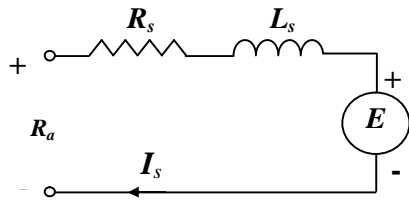


Figure A: PMSBLDC motor per phase equivalent circuit

The matrix equation for the PMSBLDC motor with three stator windings is as follows:

$$[V] = [R] * [I_s] + [L] * p * [I_s] + [E] \tag{A.1}$$

, where:

$$[V] = [V_{as} \quad V_{bs} \quad V_{cs}]^t \tag{A.2}$$

Stator phase voltage vector

$$[R] = R_s * [U] \tag{A.3}$$

Resistance matrix

, where R_s = resistance per phase, $[U]$ = Unity matrix,

$$[L] = \begin{bmatrix} L_a & L_{ba} & L_{ca} \\ L_{ba} & L_b & L_{bc} \\ L_{ca} & L_{bc} & L_c \end{bmatrix} \tag{A.4}$$

Inductance matrix

$$E = K_e w, \tag{A.5}$$

$$[I_s] = [I_a \ I_b \ I_c]^t \quad \text{Stator current vector} \tag{A.6}$$

The coupled circuit equations of the stator windings in terms of motor electrical constants are:

$$\begin{bmatrix} V_a - V_n \\ V_b - V_n \\ V_c - V_n \end{bmatrix} = \begin{bmatrix} R_s & 0 & 0 \\ 0 & R_s & 0 \\ 0 & 0 & R_s \end{bmatrix} \begin{bmatrix} I_a \\ I_b \\ I_c \end{bmatrix} + p \begin{bmatrix} L_{aa} & L_{ab} & L_{ac} \\ L_{ba} & L_{bb} & L_{bc} \\ L_{ca} & L_{cb} & L_{cc} \end{bmatrix} \begin{bmatrix} I_a \\ I_b \\ I_c \end{bmatrix} + \begin{bmatrix} E_a \\ E_b \\ E_c \end{bmatrix} \tag{A.7}$$

, where V_n is the neutral voltage.

Since the self and mutual inductances are constant (independent of the rotor position) for surface mounted permanent magnets and the winding is symmetrical, hence:

$$\begin{aligned} R_s &= R_a = R_b = R_c && \text{Stator resistance} \\ L &= L_a = L_b = L_c && \text{Self inductance} \\ M &= L_{ab} = L_{bc} = L_{ca} && \text{Mutual inductance. So,} \end{aligned}$$

$$\begin{bmatrix} V_a \\ V_b \\ V_c \end{bmatrix} = R_s \begin{bmatrix} 1 & 0 & 0 \\ 0 & 1 & 0 \\ 0 & 0 & 1 \end{bmatrix} \begin{bmatrix} I_a \\ I_b \\ I_c \end{bmatrix} + p \begin{bmatrix} L & M & M \\ M & L & M \\ M & M & L \end{bmatrix} \begin{bmatrix} I_a \\ I_b \\ I_c \end{bmatrix} + K_u \begin{bmatrix} w_a \\ w_b \\ w_c \end{bmatrix} \tag{A.8}$$

Also since $I_b + I_c = -I_a$, then, $M_{ib} + M_{ic} = -M_{ia}$, hence:

$$\begin{bmatrix} V_a \\ V_b \\ V_c \end{bmatrix} = R_s \begin{bmatrix} 1 & 0 & 0 \\ 0 & 1 & 0 \\ 0 & 0 & 1 \end{bmatrix} \begin{bmatrix} I_a \\ I_b \\ I_c \end{bmatrix} + p \begin{bmatrix} L-M & 0 & 0 \\ 0 & L-M & 0 \\ 0 & 0 & L-M \end{bmatrix} \begin{bmatrix} I_a \\ I_b \\ I_c \end{bmatrix} + K_u \begin{bmatrix} w_a \\ w_b \\ w_c \end{bmatrix} \tag{A.9}$$

Hence in State-space form,

$$\begin{aligned} \begin{bmatrix} L-M & 0 & 0 \\ 0 & L-M & 0 \\ 0 & 0 & L-M \end{bmatrix}^{-1} \text{adj} \begin{bmatrix} L-M & 0 & 0 \\ 0 & L-M & 0 \\ 0 & 0 & L-M \end{bmatrix} &= \frac{\begin{bmatrix} L-M & 0 & 0 \\ 0 & L-M & 0 \\ 0 & 0 & L-M \end{bmatrix}}{\begin{vmatrix} L-M & 0 & 0 \\ 0 & L-M & 0 \\ 0 & 0 & L-M \end{vmatrix}} = \frac{\begin{bmatrix} L-M & 0 & 0 \\ 0 & L-M & 0 \\ 0 & 0 & L-M \end{bmatrix}}{L-M \begin{bmatrix} L-M & 0 \\ 0 & L-M \end{bmatrix}} = (L-M)^{-1} (L^2 + M^2) \\ &= \frac{\begin{bmatrix} L^2 - M^2 & 0 & 0 \\ 0 & L^2 - M^2 & 0 \\ 0 & 0 & L^2 - M^2 \end{bmatrix}}{L^3 - M^3} = \begin{bmatrix} \frac{1}{L-M} & 0 & 0 \\ 0 & \frac{1}{L-M} & 0 \\ 0 & 0 & \frac{1}{L-M} \end{bmatrix} = \begin{bmatrix} \frac{1}{L_1} & 0 & 0 \\ 0 & \frac{1}{L_1} & 0 \\ 0 & 0 & \frac{1}{L_1} \end{bmatrix} \end{aligned} \tag{A.10}$$

Simplifying the Eq. A. 9, $L_1=L-M$. So,

$$\frac{d}{dt} \begin{bmatrix} I_a \\ I_b \\ I_c \end{bmatrix} = \begin{bmatrix} -\frac{R_s}{L_1} & 0 & 0 \\ 0 & -\frac{R_s}{L_1} & 0 \\ 0 & 0 & -\frac{R_s}{L_1} \end{bmatrix} \begin{bmatrix} I_a \\ I_b \\ I_c \end{bmatrix} + \begin{bmatrix} \frac{1}{L_1} & 0 & 0 \\ 0 & \frac{1}{L_1} & 0 \\ 0 & 0 & \frac{1}{L_1} \end{bmatrix} \begin{bmatrix} V_a \\ V_b \\ V_c \end{bmatrix} - \begin{bmatrix} \frac{K_u}{L_1} & 0 & 0 \\ 0 & \frac{K_u}{L_1} & 0 \\ 0 & 0 & \frac{K_u}{L_1} \end{bmatrix} \begin{bmatrix} w_a \\ w_b \\ w_c \end{bmatrix} \quad (A.11)$$

The electromagnetic torque T_e for the 3-phase BLDC motor is dependent on the current, speed and back-emf waveforms, so the instantaneous T_e can be represented as:

$$T_e = [E_a I_a + E_b I_b + E_c I_c] / w \quad [3,6] \quad (A.12)$$

The equation of motion relating rotor speed to currents, load torque, inertia and damping terms can be derived from Eq. 6 as follows:

$$dw / dt = (T_e - T_L - B_m w) / J \quad (A.13)$$

The torque equation for 3-phase PMBLDC motor can also be written as:

$$T_e = K_t I_a + K_t I_b + K_t I_c = K_t (I_a + I_b + I_c) \quad (A.14)$$

Substituting Eq. A.14 into Eq. A.13 gives the following differential equation:

$$dw / dt = [K_t (I_a + I_b + I_c) - T_L - B_m w] / J \quad (A.15)$$

A simplified term relating motor speed and torque at steady-state can be derived from the simple circuit shown in Fig. A, using Kirchoff's voltage law as follows:

$$V = I_s R + L \, dI_s / dt + E; \quad E \text{ is the induced emf per phase}$$

$$V = I_s R + K_e \omega, \quad \text{where: } E = K_e \omega \text{ and at steady-state, } dI_s / dt = 0$$

$$\omega = (V - I_s R) / K_e \quad \text{Rad/Sec}$$

$$\frac{2p N}{60} = \frac{V - R * T_e / K_t}{K_e}, \quad \text{where: } I_s = T_e / K_t \text{ and } w \text{ (Rad/Sec)} = 2p N / 60 \text{ (RPM)}$$

$$N = \frac{30}{p K_e} (V - \frac{R}{K_t} T_e) \quad \text{RPM} \quad (A.16)$$

Finally, Eq. A. 11 can be simplified in the form of state variable:

$$\dot{\mathbf{x}} = A\mathbf{x} + B\mathbf{u} + E\mathbf{w} \quad (A.17)$$

Trapezoidal Algorithm Equation:

The modification of the Euler algorithm that utilizes the sum (divided by 2) of the derivatives is evaluated at the beginning and end of the interval T . Thus,

$$x(k+1) = \frac{T_s}{2} [\dot{\mathbf{x}}(k) + \dot{\mathbf{x}}(k+1)] + x(k) \quad [9] \quad (A.18)$$

Applied to nonlinear model of Eq. 17,

$$\mathbf{x} = Ax(k) + Bu(k) + Ew(k), \text{ and } \mathbf{x}(k+1) = Ax(k+1) + Bu(k+1) + Ew(k+1) \quad (\text{A.19})$$

One way to solve the above nonlinear state equations is to transform them into a set of linear algebraic equations by employing the numerical integration methods (such as trapezoidal rule). Time discretization used for numerical integration facilitates representation of nonlinear variations in the system:

$$x(k+1) = \left(I - \frac{T_s}{2} A \right)^{-1} \left[\left(I + \frac{T_s}{2} A \right) x(k) + \frac{T_s}{2} B [u(k+1) + u(k)] + \frac{T_s}{2} E [w(k+1) + w(k)] \right] \quad (\text{A.20})$$

, where for the 3-phase PMBLDC motor model:

$x = I_a, I_b$ and I_c , $u = V_a, V_b$ and V_c and $\omega = \omega_a, \omega_b$, and ω_c

$I =$ identity matrix, and A, B , and E is as follow in state-space model.

$k =$ numbers of time intervals and $T_s =$ small intervals time.